HHS Public Access

Author manuscript

Nat Neurosci. Author manuscript; available in PMC 2020 October 20.

Published in final edited form as:

Nat Neurosci. 2020 May ; 23(5): 611–614. doi:10.1038/s41593-020-0623-9.

Primate auditory prototype in the evolution of the arcuate fasciculus

Fabien Balezeau[1,a], **Benjamin Wilson**[1,a], **Guillermo Gallardo**[2], **Fred Dick**[3], **William Hopkins**[4], **Alfred Anwander**[2], **Angela D. Friederici**[2], **Timothy D. Griffiths**[1,5,6,b], **Christopher I. Petkov**[1,b]

[1]Newcastle University Medical School, Newcastle upon Tyne, UK

[2]Max Planck Institute for Cognitive and Brain Sciences, Department of Neuropsychology, Leipzig, Germany

[3]Birkbeck UCL Centre for NeuroImaging (BUCNI), Birkbeck University of London, UK

[4]University of Texas Keeling Center for Comparative Medicine and Research, USA

[5]Wellcome Trust Centre for Neuroimaging, University College London, UK

[6]Department of Neurosurgery, University of Iowa, Iowa City, USA

Abstract

The human arcuate fasciculus pathway is crucial for language, interconnecting posterior temporal and inferior frontal areas. Whether a monkey homolog exists was controversial and the nature of human-specific specialization unclear. Using monkey, ape and human auditory functional fields and diffusion MRI, we identified homologous pathways originating from auditory cortex. This discovery establishes a primate auditory prototype for the arcuate fasciculus, reveals an earlier phylogenetic origin and illuminates its remarkable transformation.

The human Arcuate Fasciculus (AF) is a dorsal brain pathway critical for language[1]. It matures during childhood into a dominant and left hemisphere lateralized pathway[2], damage to which results in language disorder[3]. Insights on AF evolution are important for understanding the emergence of language and human-specific brain specialization.

Chimpanzees (an ape species) possess an AF homolog interconnecting posterior temporal and inferior frontal areas, but the extent to which macaques (a monkey species) have a similar pathway is controversial[4–8,9] (Fig. 1A). Current accounts[7,10,11] link AF evolutionary

Corresponding authors: fabien.balezeau@newcastle.ac.uk.
Present addresses: BW: Department of Psychology at Emory University and Yerkes National Primate Research Center, USA.
[a.]Joint first authors (FB & BW);
[b.]Joint senior authors (TDG & CIP)

Author Contributions

Study conception: CIP, FB, ADF & TDG; Conducted study and analysis: FB, BW, GG, FD, AA, CIP; Provided materials: FB, BW, GG, FD, WH, AA, ADF, TDG & CIP; Wrote paper: CIP, FB, BW, with revision from coauthors GG, FD, WH, AA, ADF & TDG.

Accession codes: Open Science Framework https://osf.io/arqp8/. Also see Methods and Life Science Reporting Summary.

Competing Financial Interests Statement

The authors declare no competing financial interests.

differentiation with expansion of the Middle Temporal Gyrus (MTG), a prominent gyrus in humans that is evident in chimpanzees but not monkeys[6,7,10]. It follows that MTG projections to inferior frontal cortex via an AF homolog, if present in ape and human common ancestors, would not be unique to modern humans or language. Further human differentiation of MTG and AF is expected to coincide with language evolution, but the nature and evolutionary context of human-specific AF specialization remained poorly understood.

Here, we address the question of whether a monkey fronto-temporal homolog of the AF might exist, despite the absence of an MTG in monkeys. We do this by *functionally* defining the likely origin of an auditory segment of this pathway in rhesus macaques, chimpanzees and humans, using auditory tonotopic information and probabilistic diffusion MRI tractography. Projection patterns from auditory cortex in monkeys, although often assumed to rely on a ventral rather than dorsal pathway, required direct comparison to other primates. It was also unclear the extent to which prior comparative neuroimaging studies compared temporal lobe areas across the species with different function (i.e., auditory, visual or associative) and thus different connectivity (Fig. 1A). We demonstrate that a symmetrical auditory evolutionary prototype of the human AF originating in the auditory cortex exists in both macaques and chimpanzees and that a critical evolutionary lateralization of this pathway occurred in humans.

First, we leveraged an openly available ultra-high resolution (200μm) post-mortem macaque dMRI dataset[12]. Exploratory analyses revealed considerable dorsal pathway connections between posterior supratemporal areas and inferior frontal cortex in both hemispheres (Fig. 1B).

Next, given that humans are often studied awake during dMRI, we worked to collect original awake dMRI datasets in three macaques (5 scans and ~75 min per animal), informed by an fMRI probabilistic tonotopic map obtained in several macaques to approximate the location of Auditory Cortical Fields (ACFs; Online Methods). To determine which ACFs project to inferior frontal cortex and whether by ventral or dorsal pathways, ACF ROIs (Fig. 1C) were used as seeds in deterministic (see Extended Data Fig. 1) and probabilistic analyses, corrected for partial-volume effects and spurious dorsal pathway projections (Methods, Extended Data Fig. 2). In all three macaques, the ventral pathway was prominent from more anterior ACFs (Fig. 1D–E). However, a clear dorsal pathway to inferior frontal cortex was also found, arising particularly from postero-medial ACFs (e.g., fields MM, A1, CM). Comparing coronal sections to a standard macaque atlas on fiber pathways[13] shows that this dorsal auditory pathway involves the macaque AF homolog and portions of the Superior Longitudinal Fasciculus (SLF) II/III (Extended Data Fig. 3). We quantified effects using dorsal and ventral waypoint analyses (Fig. 1E). Testing these macaque data showed a dorsal vs. ventral pathway effect (RM-ANOVA, $p = 0.003$; Online Methods) but no hemisphere effect or interaction with pathway and hemisphere.

In chimpanzees, we conducted similar analyses on dMRI datasets in three animals scanned anesthetized after a regular veterinary check-up (Methods). We used three anatomically defined auditory ROIs based on prior tonotopic results in apes[14] and the location of the

chimpanzee Heschl's gyrus (auditory cortex) homolog (Fig 2A). As in macaques, probabilistic tractography identified ventral and dorsal pathways in the chimpanzees (Fig 2A). As with macaques, both ventral and dorsal projections from auditory seed regions were largely symmetrical across the hemispheres (Methods). This result differs from previous evidence of ape dorsal pathway projections from broader temporal lobe sites including association and visual cortical areas, which are left lateralized as in humans[10].

In humans, we used ACF seeds from human tonotopic fMRI maps (Fig. 2B) to analyze three dMRI datasets. Probabilistic tractography replicated previous findings, showing more pronounced dorsal versus ventral pathways (Fig 2C–D), and we identified an auditory segment of the human AF. In contrast to the observations in macaques and chimpanzees, the auditory segment of the human AF appears left lateralized, particularly from postero-medial ACFs (compare with[15]). We found a significantly stronger dorsal vs ventral pathway effect ($p = 0.031$) and a statistical trend in the left hemisphere effect and interaction with pathways as a factor (both $p < 0.06$; Online Methods).

Finally, we quantified and compared the connectivity of the auditory cortex projections from both pathways in all three species. In line with previous findings, the ventral pathway is predominant in macaques and chimpanzees, with the dorsal predominating in humans (cross-species RM-ANOVA showed a species and pathway interaction, $p = 0.003$). We also observed a significant interaction of species, pathway and hemisphere ($p = 0.002$) driven by the left lateralized human auditory cortex dorsal pathway (Fig. 3) relative to the more symmetrical pattern in apes and monkeys.

This work provides new insights on the evolutionary origins of the AF. It establishes an auditory segment of the human AF and provides evidence for homologous pathways in chimpanzees and macaques. The auditory dorsal pathway's lack of strong asymmetry in nonhuman primates is in stark contrast to the left hemisphere asymmetry seen in humans here and elsewhere[15]. The findings advance an intriguing explanatory account of human arcuate fasciculus evolution, addressing 1) the evolutionarily conserved primate prototype, 2) when it may have emerged, and 3) human-specific differentiation.

Current accounts of human AF evolution[7,10,11] are based on evolutionary changes predating human language evolution, thought to have begun to take form in ape and human ancestors (Fig. 1A). A key evolutionary change is often linked to the presence of the MTG in apes and the further expansion of AF connectivity from it in human ancestors[7]. This account often assumes a greater visual role of the macaque dorsal pathways, e.g., monkey dorsal pathway projections from parietal cortex[11]. Given that chimpanzee dMRI had previously shown left-hemisphere asymmetry in the dorsal pathway from other temporal lobe areas[10], it could previously be assumed that all the pieces began to take form in ancestors to apes and humans, followed by further differentiation in human ancestors.

The current results advance a *primate auditory prototype* hypothesis, raising the possibility that our shared ancestors with apes and monkeys possessed symmetrical dorsal pathways interconnecting auditory temporal lobe regions with inferior frontal cortex (Fig. 3). The left hemisphere auditory AF connectivity pattern in humans appears to have differentiated

further from this primate auditory prototype. The hypothesis also posits a key point of differentiation that appears to have occurred uniquely in the human lineage: the differentiation of the human *right* dorsal pathway connectivity away from the auditory prototype to involve more caudal temporal and parietal areas[15].

The contribution to the dorsal pathway from auditory areas is interesting and perhaps surprising, in that an evolutionarily conserved system relies on relatively early stage auditory cortical input via ventral and dorsal pathways. In macaques, anterograde tractography has shown that prefrontal cortex receives monosynaptic auditory input from belt auditory cortex[16]. Our dMRI observations across the species now identify the auditory segment of the dorsal pathway and push back the emergence of the auditory prototype of the AF further than the split from a common ancestor with macaques (~25 million years ago), rather than the previously assumed 5 million years ago when humans and chimpanzees last shared a common ancestor.

Our observations fit with the notion that language adaptations may have arisen from primate auditory pathways[17]. We speculate that this dorsal auditory pathway is involved in not just spatial processing in the classical sense but also sound and vocal patterning in the time domain[18], which is supported by evidence implicating inferior frontal cortex in sound sequence patterning in macaques and humans[19] and vocalization sound processing and production in macaques, marmosets and humans[20]. Whereas auditory processes in monkeys may have previously been assumed to involve ventral pathways, the current results in macaques indicate that a dorsal auditory pathway should not be dismissed. Future studies could assess the extent to which New World monkeys, prosimians or even non-primate species might have an auditory dorsal pathway to inferior frontal cortex, to pinpoint its earliest evolutionary origin.

ONLINE METHODS

Diffusion MRI datasets overview

The post-mortem macaque ultra high-resolution diffusion dataset was obtained via an openly shared resource[12]. The dMRI datasets in the three awake male macaques were obtained as described below, with a probabilistic fMRI tonotopic map based on[21,22]. The dMRI scans of three anesthetized male chimpanzees were obtained via the National Chimpanzee Brain Resource (http://www.chimpanzeebrain.org), with auditory cortex location as detailed below. The awake adult human diffusion datasets were obtained from an openly shared resource[24], with an fMRI tonotopic map based on[25].

Macaque awake datasets

Diffusion-weighted MRI scans were acquired in three adult male rhesus macaques (macaca mulatta): M1, M2 and M3 weighing respectively 10kg, 16kg and 12kg and aged 10, 13 and 7. The three macaques were visually assessed for their preferred hand when grasping objects (e.g., food): M1 and M3 were mostly bimanual showing no preference for hand of use, and M2 showed a right hand preference. There was no obvious relationship with handedness in the macaque results.

All procedures conducted with the macaques were approved by the Animal Welfare and Ethical Review Body (AWERB) and the UK Home Office and are in full compliance with both the UK Animal Scientific Procedures Act (ASPA) and the European Directive (2010/63/EU) on the care and use of animals in research. We support the principles of the consortium on Animal Research Reporting of In Vivo Experiments (ARRIVE). Given the ethical sensitivities involved in research with nonhuman primates and the 3Rs principles (one of which is on the Reduction of animal numbers), our work with awake behaving macaques requires using the fewest macaques necessary. A sample size of two to three is common in behavioral neuroscience experiments with macaques provided that results are robust within each individual and that the effects generalize beyond one animal, as they do (see manuscript). Training macaques for awake MRI scanning requires a substantial time investment, and the data that was combined for each of these datasets in each of the three animals are robust, consistent across the three animals, and the same sample size in chimpanzees and humans allowed cross-species comparisons. Thus there was little ethical justification to train and test additional monkeys.

Awake macaque diffusion-weighted MRI procedure

The macaques were scanned sitting in a primate chair within a vertical MRI scanner (Biospec 4.7 Tesla, Bruker Biospin, Ettlingen, Germany). The macaques had all been previously acclimatized to the scanner environment and to the length of scanning required, and they were trained for an fMRI scanning task including periodic fixation under head immobilization using operant training[19]. The macaques were rewarded with juice for fixating a central spot on the screen for 2–4s, as measured with an infra-red eye tracker; ISCAN, Inc.

A 4 channel receiver surface coil array and a saddle transmitter coil were used for MRI acquisition (WK Scientific, San Diego, California). The sequence used was diffusion weighted (DW) spin echo (SE) echo planar imaging (EPI) with the following parameters: TE = 58ms, TR = 14,200ms, matrix 88 × 88, 56 slices, for a voxel size of 0.97mm × 0.97mm × 1mm. Two-fold GRAPPA (GeneRalized Autocalibrating Partial Parallel Acquisition) acceleration was applied to obtain low distortion, high resolution and motion-robust acquisition. *B0* field uniformity was optimized using the MAPSHIM algorithm along 1st and 2nd order shim gradients (Bruker, Ettlingen, Germany). To provide the best possible fiber discrimination and tracking, we used a High Angular Resolution Diffusion Imaging (HARDI) approach with the highest spatial resolution enabled by the hardware at 4.7T. We acquired 60 diffusions directions (b=850s/mm2) and four b=0 images. The scan was repeated 5 times to improve signal to noise ratio. The total scan duration was ~75min for each subject. Saturation slices were used to suppress signal from the temporal muscles, eyes and mouth. This also enabled us to reduce the field of view and thus increase the scanning resolution. A fat suppression preparation pulse was applied to reduce ghosting artefacts.

Awake macaque diffusion data processing

Deterministic (dMRI) was performed using the BioImage Suite (Yale, USA). Deterministic tracking (see Extended Data Fig. 1) was used primarily for visualization purposes, since the result will always follow the largest dominant fractional anisotropy (FA) values. However,

deterministic tracking has a high false negative rate and there was no clear evidence in any but one of the animals of a dorsal pathway with this approach (Extended Data Fig. 1): Two ventral pathways were consistently observed in every animal, medially (Extreme Capsule and Uncinate Fasciculus pathways, EC/UF) and laterally (MdLF: Middle Longitudinal Fasciculus) interconnecting anterior ACFs with other temporal lobe sites and inferior frontal cortex. Cross-callosal connections and those to parietal cortex, auditory thalamus (MGN) and inferior colliculus were also observed using this approach in the majority of the animals.

The FSL Toolbox[26] FDT tool (6.0.1) was used to compute a more complex diffusion model and to perform probabilistic fiber tracking[27]. Diffusion parameters were computed using BEDPOSTX with default settings (2 fibers, weight 1). Fiber tracking was performed by PROBTRACKX using default setting (5000 samples, curvature threshold=0.2), with a given Region-Of-Interest (ROI) mask as seed region. Probabilistic tracking for a given seed voxel or region provides a connectivity index map in the form of streamline (fiber) count for each voxel.

Seed regions for fiber tracking were defined based on Auditory Cortical Field (ACF) tonotopic mapping along the superior temporal plane[21,22]. ACF regions of interests included auditory core (A1, R, RT) and belt areas (CL, CM, ML, MM, AL, AM, RTL, RTM) drawn from a volumetric probabilistic tonotopic map defined from majority overlap in ACF locations in a co-registered group of 10 macaques scanned awake over the last 10 years. The probabilistic map was registered to the individual native-space dMRI fractional anisotropy maps for each subject.

All ROI voxels were inspected for partial volume effects and anatomical structure mis-registration, correcting if needed ROI overlap or anatomical involvement of non-auditory regions prior to further analysis. We excluded voxels in the superior temporal sulcus or the dorsal bank of the lateral sulcus. The ACF ROIs were also restricted to gray matter using the FSLs FAST white matter segmentation tool as a white matter exclusion mask[26]. To avoid artefactual dorsal pathway voxels not emanating from the auditory cortex, a volumetric exclusion mask was defined covering the full extent of the sylvian fissure (lateral sulcus) separating the superior temporal plane and dorsal regions in frontal and parietal cortex (Extended Data Fig. 2). Omission of this mask causes strong false positive dorsal pathways involvement because some auditory cortex voxels in the superior temporal plane are mislocalized to the dorsal lateral sulcus owing to partial volume effects. The lateral sulcus exclusion mask ensures that the analyses are more conservative with regards to spurious dorsal supra-temporal plane to inferior frontal cortex pathway connectivity.

Dorsal and ventral waypoints were defined as ROIs for comparing the relative strength of the pathways based on the probabilistic tracking results in each animal (Fig. 1D). For each functionally defined seed ACF region (e.g., A1, CM etc) the mean connectivity index value was extracted from the voxels in these anatomically defined ROIs. Connectivity measurements (fiber count) are shown and used for further analysis as indicated. Figure 1C and E do not show the more rostral ACFs (RTM, RT and RTL) because these regions do not show dorsal pathway projections. Fig. 1E shows the normalized connectivity from each ACF via the dorsal and ventral pathway, in each hemisphere. Macaque 3 had low SNR in one

hemisphere that may be implant related and could not be avoided, affecting the dorsal pathway in the left hemisphere. Therefore, to avoid suggesting spurious right lateralization effects these data were omitted from the illustrative heat map summary in (Fig. 1E) but are included in the other analyses. The connectivity results are displayed on a model of auditory cortical fields (Fig. 1E) and rendered on the cortical surface (Extended Data Fig. 4).

Statistics.—We used repeated-measures (RM) ANOVA models to test the relative connectivity between inferior frontal and auditory cortex in the left and right hemispheres: Within-subjects factors of Pathway (dorsal, ventral), Hemisphere (left, right). The results for the macaque model ($n = 3$ animals) showed a main effect of Pathway ($F_{1,2} = 211.4$, $p = 0.005$), indicating a stronger ventral than dorsal pathway, but no main effect of Hemisphere ($F_{1,2} = 4.06$, $p = 0.181$) or interaction ($F_{1,2} = 0.294$, $p = 0.642$). The data and variance distributions of this model fit the assumptions of the analysis. The data and variance distributions of this model fit the assumptions of the analysis. No statistical methods were used to pre-determine sample sizes but our sample sizes are similar to those previously used[6–9,12,13,16,19]. Data collection could not be blinded to species or individuals, but the analyses used pre-defined seed regions and waypoint crossings and were conducted in the same way agnostic to the conditions being analyzed. Please see Life Sciences Reporting Summary.

Chimpanzee dMRI analyses

The chimpanzee datasets were provided already preprocessed with FSL BEDPOSTX (http://www.chimpanzeebrain.org). The three male chimpanzees (aged 15, 20 and 21 years old) had been visually assessed for their hand of preference. C1 and C2 had a preference for using the right hand. C3 had a left hand preference. There was no obvious relationship with handedness in the chimpanzee results.

Fiber tracking was performed using PROBTRACKX using default settings with a given auditory ROI mask as seed region. Three auditory cortical areas were defined by placing ROIs over the chimpanzee transverse temporal gyrus, the center of the presumed homolog of the human Heschl's Gyrus[12,29], and two regions either posterior or anterior to it of similar size, all restricted to gray matter (Fig. 2A). Unlike the macaques, a lateral sulcus exclusion mask was not necessary given the larger ape brain and the greater separation of dorsal and ventral banks of the lateral sulcus, naturally reducing partial volume effects. The volumetric ROIs were restricted to the gray matter and distanced from the lateral sulcus by at least a voxel to prevent tracking via non-auditory regions dorsal to auditory cortex.

Statistics.—Statistical testing of the dorsal versus ventral and left versus right fiber counts across the three chimpanzees used RM-ANOVA: Within-subjects factors of Pathway (dorsal, ventral), Hemisphere (left, right). The data and variance distributions fit the assumptions of the analysis. In the chimpanzee model ($n = 3$ animals), we observed no significant effects of Pathway ($F_{1,2} = 3.33$, $p = 0.0.209$), Hemisphere ($F_{1,2} = 0.104$, $p = 0.778$) or higher order interactions between these factors ($F_{1,2} = 11.773$, $p = 0.075$). No statistical methods were used to pre-determine sample sizes but our sample sizes are similar to those previously used[7,14,29]. Data collection could not be blinded to species or individuals, but the analyses

used pre-defined seed regions and waypoint crossings and were conducted in the same way agnostic to the conditions being analyzed. Please see Life Sciences Reporting Summary.

Human dMRI analyses

Three male subjects between 25 and 32 years old were randomly selected from the group S500 of the Human Connectome Project (HCP). All the subjects were already preprocessed with the HCP minimum pipeline. Auditory ROIs were based on a combination of frequency band activity preferences and estimated myelin map discontinuities (N=55) in cross-subject surface-based averages defined on the cortical surface of an individual subject whose brain had been morphed to the MNI atlas before surface reconstruction in FreeSurfer. ACF ROIs are shown in Figure 2B, overlaid on the average tonotopic map of the right hemisphere. The two 'auditory core' ROIs (ACF numbers 5 and 8 in Fig. 2C) were defined within a patch of maximal R1 intensity and delineated by higher and lower frequency preferences. The other 'Belt/Parabelt' ROIs were defined from the medial and lateral borders of anterior auditory core: The Anterior ROI (1 in Fig. 2B) was more weakly tonotopic on average, and it straddled a low-to-medium frequency preference region. The more lateral ROI was a patch with lower-frequency preference along the STG (2 in Fig. 2B), and the more medial one was within a higher-frequency preference region (7 in Fig. 2B). The Posterior Belt/Parabelt ROIs (6 and 4 in Fig. 2B) straddled the posterior aspect of the core field (5 and 8) and showed high-frequency preference. The Posterolateral ROI (3 in Fig. 2B) encompassed a tonotopic region with middle-frequency preference lateral to the R1 hyperintense band notable along the STG.

Each ROI was surface-morphed from the individual subject to FreeSurfer's fsaverage, and was then projected into the cortex (from 10% below the white/grey border to the pial surface) of the 2mm isotropic resolution MNI 152 volume. The three human subjects were registered to MNI space using a non-linear registration algorithm (FSL's FLIRT and FNIRT). Then, the inverse transform was applied to each volumetric ROI to bring them into each subjects' space. To estimate the connectivity of each ROI to inferior frontal cortex, volumetric probabilistic tractography was performed using the Constrained Spherical Deconvolution[30] implementation on MRTRIX (1000 streamlines option).

Statistics.—As in the macaques and chimpanzees, we conducted an RM-ANOVA with the within-subjects factors of Hemisphere (left and right) and Pathway (dorsal and ventral). The data and variance distributions fit the assumptions of the analysis. In humans (n = 3), we observed a main effect of Pathway ($F_{1,2}$=30.6, p=0.031), with the dorsal pathway stronger than the ventral. There was also a left hemisphere trend seen for Hemisphere ($F_{1,2}$=15.8, p=0.058) and Hemisphere and Pathway ($F_{1,2}$=15.7, p=0.058). No statistical methods were used to pre-determine sample sizes but were matched to the numbers available in macaques and chimpanzees. Data collection could not be blinded to species or individuals, but the analyses used pre-defined seed regions and waypoint crossings and were conducted in the same way agnostic to the conditions being analyzed. Please see Life Sciences Reporting Summary.

Cross-species statistical comparisons

An RM-ANOVA model was implemented with all the dMRI data for the three-way cross species comparison with the following factors: Within subjects factors of Pathway (dorsal, ventral), Hemisphere (left, right); Between subjects factor of Species (macaque, chimpanzee, human). The analysis showed an interaction of Species and Pathway ($F_{2,6}$=18.1, p=0.003) reflecting the relatively larger dorsal pathway in humans and ventral pathways in monkeys and apes (see Fig. 3). There was also an interaction of Species, Pathway and Hemisphere ($F_{2,6}$=20.7, p=0.002), driven by the left lateralization of the human dorsal pathway relative to the more symmetrical pathways in the other species. No other effects or interactions were significant.

Data Availability and Accession Code Availability Statements

The ultra-high resolution post mortem macaque dataset is from a previously shared resource. The chimpanzee and human datasets are from available resources (http://www.chimpanzeebrain.org, group S500 of the Human Connectome Project). The awake macaque dMRI data is available from Open Science Framework, accession site (https://osf.io/arqp8/) and will be made available in the primate MRI open data sharing resource (PRIME-DE: http://fcon_1000.projects.nitrc.org/indi/indiPRIME.html). The regions of interest are available in available atlases or as part of prior publications.

Code Availability: custom code and analyses were not required. Available analysis pipelines used FSL (FDT v. 6.0.1) and other processing pipelines as noted.

Extended Data

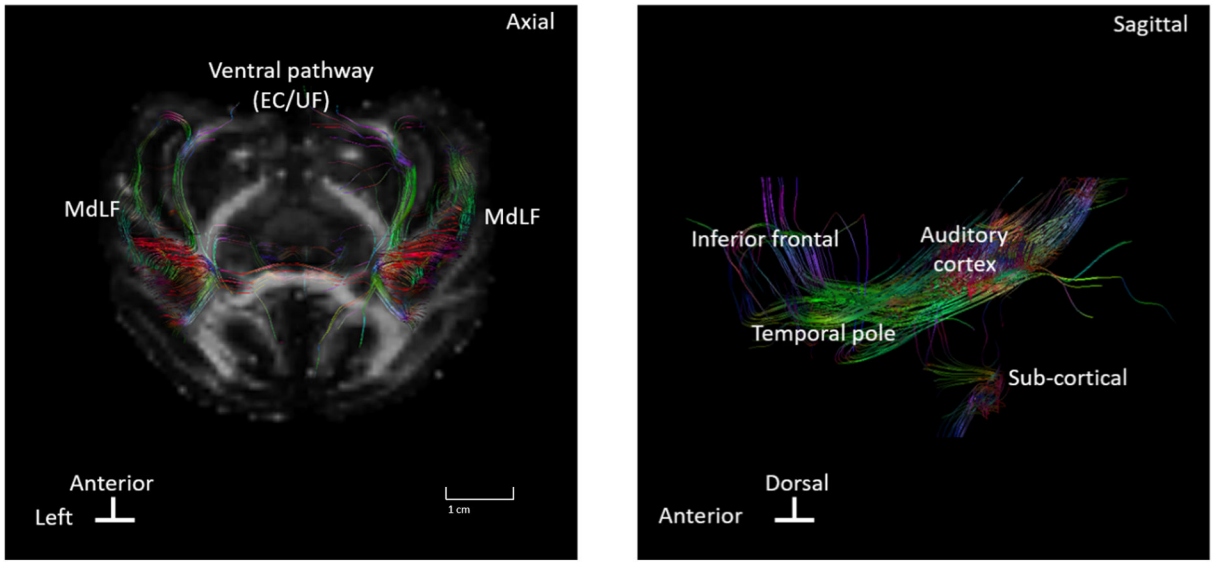

Extended Data Fig. 1. Macaque deterministic tractography

Axial (left) and sagittal (right) slices showing diffusion weighted fractional anisotropy (FA) map overlaid with deterministic tractography. The sagittal slice shows the auditory pathways coursing to inferior frontal cortex via a ventral pathway medially involving the Uncinate Fasciculus/Extreme Capsule (UF/EC) pathway and laterally via the Middle Longitudinal Fasciculus (MdLF). No clear dorsal pathway from auditory cortex is observed using deterministic tractography. Diffusion directions, green: anterior-posterior; blue: dorsal-ventral; red: medial-lateral.

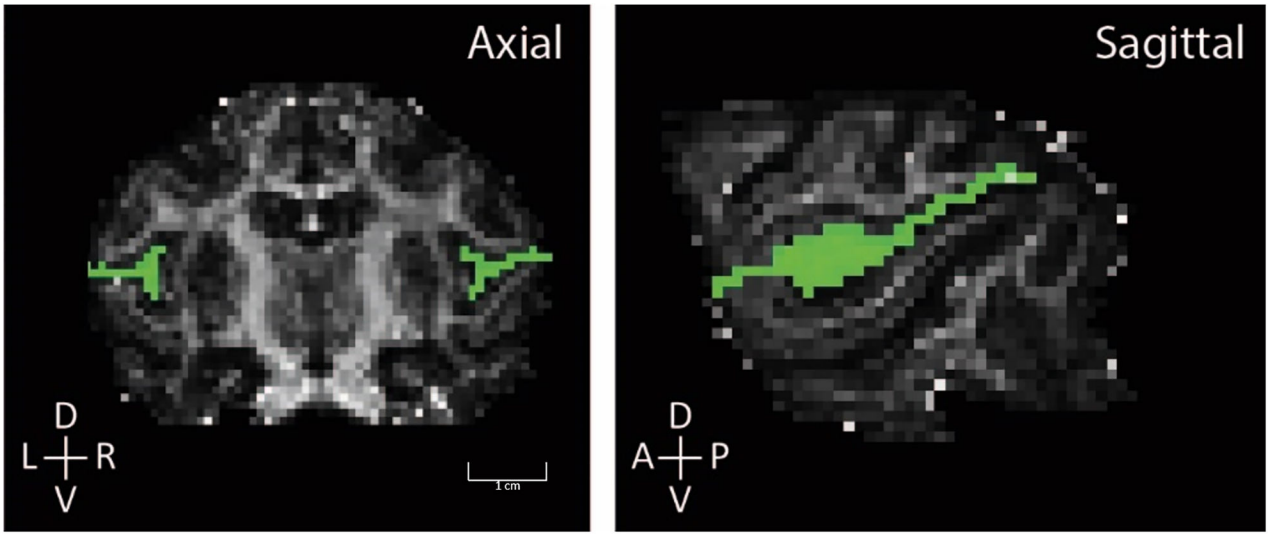

Extended Data Fig. 2. Lateral sulcus exclusion mask in the macaques

To avoid artefactual dorsal pathway voxels not emanating from auditory cortex, an exclusion mask covering the full extent of the Sylvian fissure (lateral sulcus) separating the superior temporal plane and dorsal regions in frontal and parietal cortex was defined. Omission of this mask causes strong false positive dorsal pathways involvement because some auditory cortex voxels in the superior temporal plane are mislocalized to the dorsal lateral sulcus owing to partial volume effects. The lateral sulcus exclusion mask ensured that the analyses are more conservative with regards to spurious dorsal supra-temporal plane to inferior frontal cortex pathway connectivity.

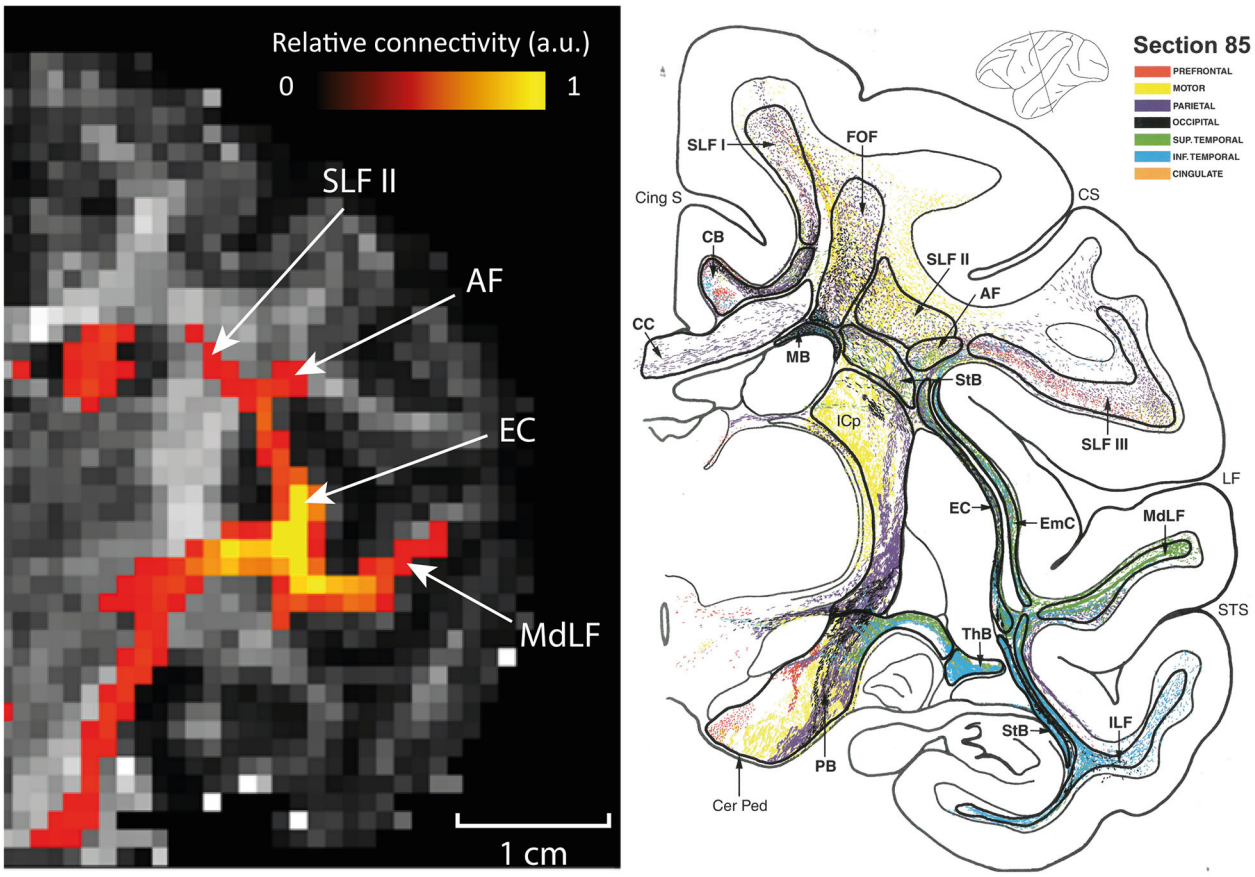

Extended Data Fig. 3. Example comparison of probabilistic dMRI to a macaque fibre pathways atlas coronal section

Comparison of one of the coronal slices (left) showing tractography from the MM seed region, with a similarly located coronal section (right) from the Schmahmann and Pandya macaque brain pathways atlas[13] (copyright permission obtained from Oxford Publishing Limited), suggests that the dorsal pathways that we observed involve the macaque AF and parts of the Superior Longitudinal Fasciculus (SLF). SLF II: Superior Longitudinal Fasciculus II; AF: Arcuate Fasciculus; EC: Extreme Capsule pathway (Uncinate Fasciculus is visible on more anterior coronal sections); MdLF: Middle Longitudinal Fasciculus.

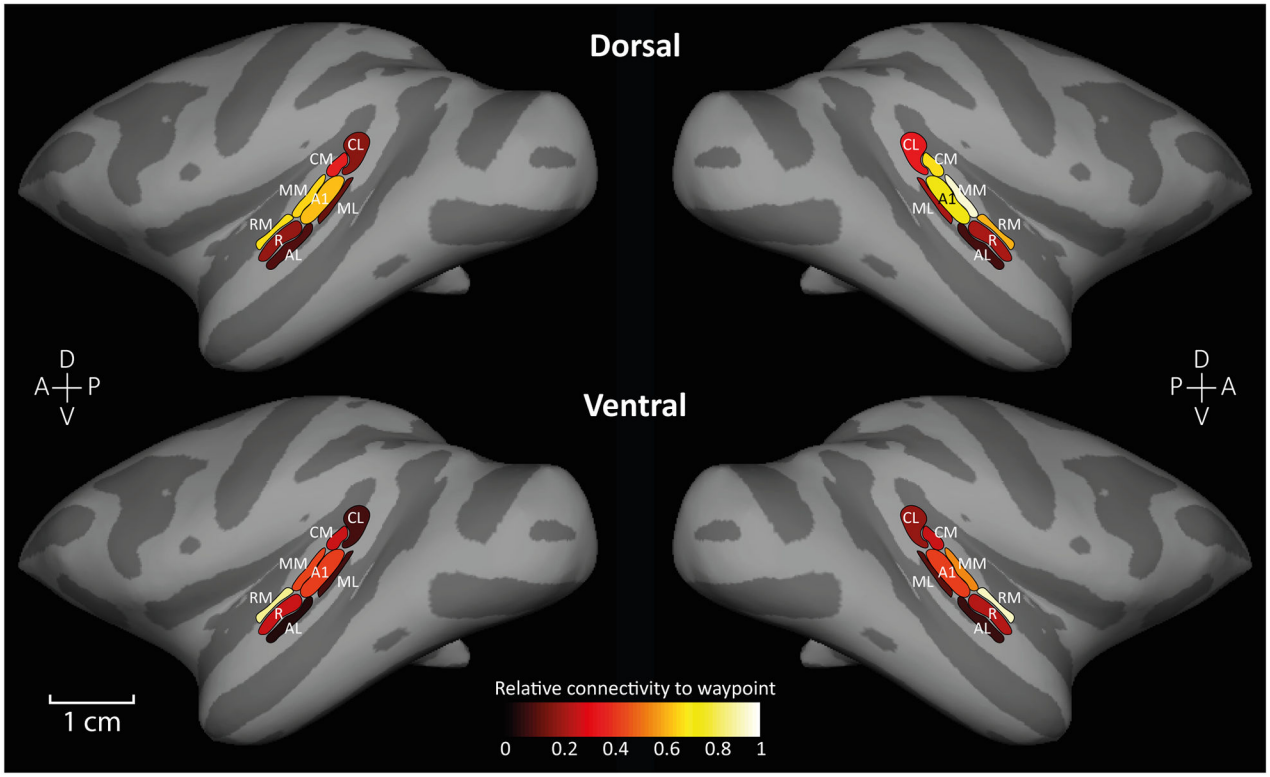

Extended Data Fig. 4. Mean relative connectivity heat maps for each macaque auditory cortical field

Showing mean relative dorsal and ventral connectivity from each ACF (from Fig. 1E) rendered on the cortical surface for closer comparison with the human results (Fig. 2D).

Supplementary Material

Refer to Web version on PubMed Central for supplementary material.

Acknowledgements

We thank N. Eichert, R. Mars, A. Mitchell and M. Rushworth for excellent discussion. Support: Wellcome Trust (TDG: WT091681MA; CIP: WT092606AIA; BW: WT110198); Max Planck Society (ADF & AA); European Research Council (CIP: MECHIDENT); National Institutes of Health (Matthew Howard III with TDG and CIP: R01-DC04290).

REFERENCES

1. Hagoort P Science 366, 55–58 (2019). [PubMed: 31604301]
2. Anwander A et al. Cerebral Cortex 17, 816–825 (2006). [PubMed: 16707738]
3. Price CJ et al. Neurology 6, 202–210 (2010). [PubMed: 20212513]
4. Bornkessel-Schlesewsky I et al. Proceedings National Acad. of Sciences 19, 142–150 (2015).
5. Skeide MA & Friederici AD. Trends in Cognitive Sciences 19, 483 (2015). [PubMed: 26094088]
6. Thiebaut de Schotten M et al. Cortex 48, 82–96 (2012). [PubMed: 22088488]
7. Rilling JK et al. Nature Neurosci 11, 426–428 (2008). [PubMed: 18344993]
8. Eichert N et al. Cortex 118, 107–115 (2018). [PubMed: 29937266]
9. Frey S et al. Brain Language 131, 36–55 (2014). [PubMed: 24182840]

10. Rilling J et al. Frontiers Evolutionary Neuroscience 3, 11 (2012).
11. Mars RB et al. Current Opinion in Behavioral Sciences 21, 19–26 (2018).
12. Calabrese E et al. NeuroImage 117, 408–416 (2015). [PubMed: 26037056]
13. Schmahmann J & Pandya D. Fiber Pathways of the Brain (OUP USA, 2009).
14. Bailey P et al. Journal of Neurophysiology 6, 121–128 (1943).
15. Takaya S et al. Frontiers Neuroanatomy 9, 119 (2015).
16. Romanski LM et al. Nature Neuroscience 2, 1131–1136 (1999). [PubMed: 10570492]
17. Rauschecker JP & Scott SK. Nature Neuroscience 12, 718–724 (2009). [PubMed: 19471271]
18. Zhang YS & Ghazanfar AA. Trends in Neurosciences 42: P115–126 (2020).
19. Wilson B et al. Nature Communications 6, 8901 (2015).
20. Flinker A & Knight RT. Current Opinion in Behavioral Sciences 21, 170–175 (2018).
21. Petkov CI et al. PLoS Biology 4, e215 (2006). [PubMed: 16774452]
22. Baumann S et al. NeuroImage 50, 1099–1108 (2010). [PubMed: 20053384]
24. Van Essen DC et al. NeuroImage 62, 2222–2231 (2012). [PubMed: 22366334]
25. Dick F et al. J. Neuroscience 32, 16095–16105 (2012).
26. Smith SM et al. NeuroImage 23 Suppl 1, S208–219 (2004). [PubMed: 15501092]
27. Behrens TEJ et al. Magnetic Resonance in Medicine 50, 1077–1088 (2003). [PubMed: 14587019]
28. Zhang Y et al. IEEE Transactions on Medical Imaging 20, 45–57 (2001). [PubMed: 11293691]
29. Hackett TA et al. Journal of Comparative Neurology 441, 197–222 (2001). [PubMed: 11745645]
30. Tournier J-D, et al. NeuroImage 35, 1459–1472 (2007). [PubMed: 17379540]

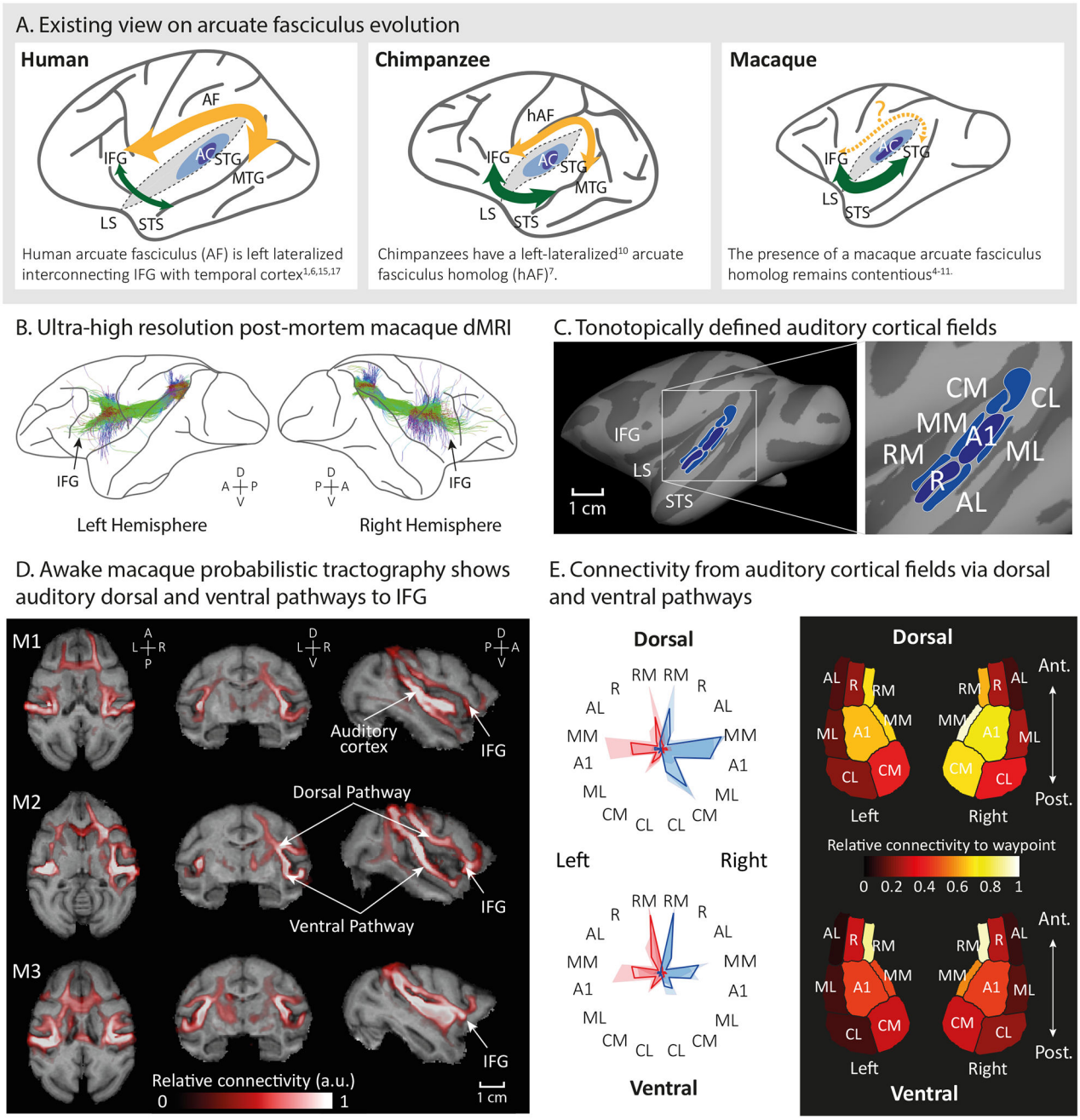

Figure 1. Existing view and evidence for monkey dorsal and ventral auditory pathways.

(A) Illustration of an existing view on arcuate fasciculus evolution originating with a common ancestor to humans and chimpanzees, see text. Dashed lines illustrate an expanded lateral sulcus (LS) showing the location of auditory cortex on the superior temporal plane. (B) Deterministic tractography in the ultra-high resolution *ex-vivo* macaque dMRI dataset[12]. Diffusion directions, green: anterior-posterior; blue: dorsal-ventral; red: medial-lateral. (C) fMRI tonotopically defined core (dark blue) and belt (light blue) ACFs, each of which is based on a gradient of low to high frequency selectivity. (D) Awake macaque probabilistic tractography (relative connectivity arbitrary units, a.u.) showing dorsal and ventral

connections between inferior frontal cortex and a postero-medial auditory cortical field (MM). (E) Mean relative connectivity fingerprints (thick lines) and individual variability (shaded) in the left (red) and right hemisphere (blue); shown on a model of ACFs as heat maps (right panel), also see Extended Data Fig. 4. Abbreviations; AC: auditory cortex; AF: arcuate fasciculus; hAF: homolog of arcuate fasciculus; IFG: inferior frontal gyrus; LS: lateral sulcus; MTG: middle temporal gyrus (not present in macaques); STG: superior temporal gyrus; STS: superior temporal sulcus.

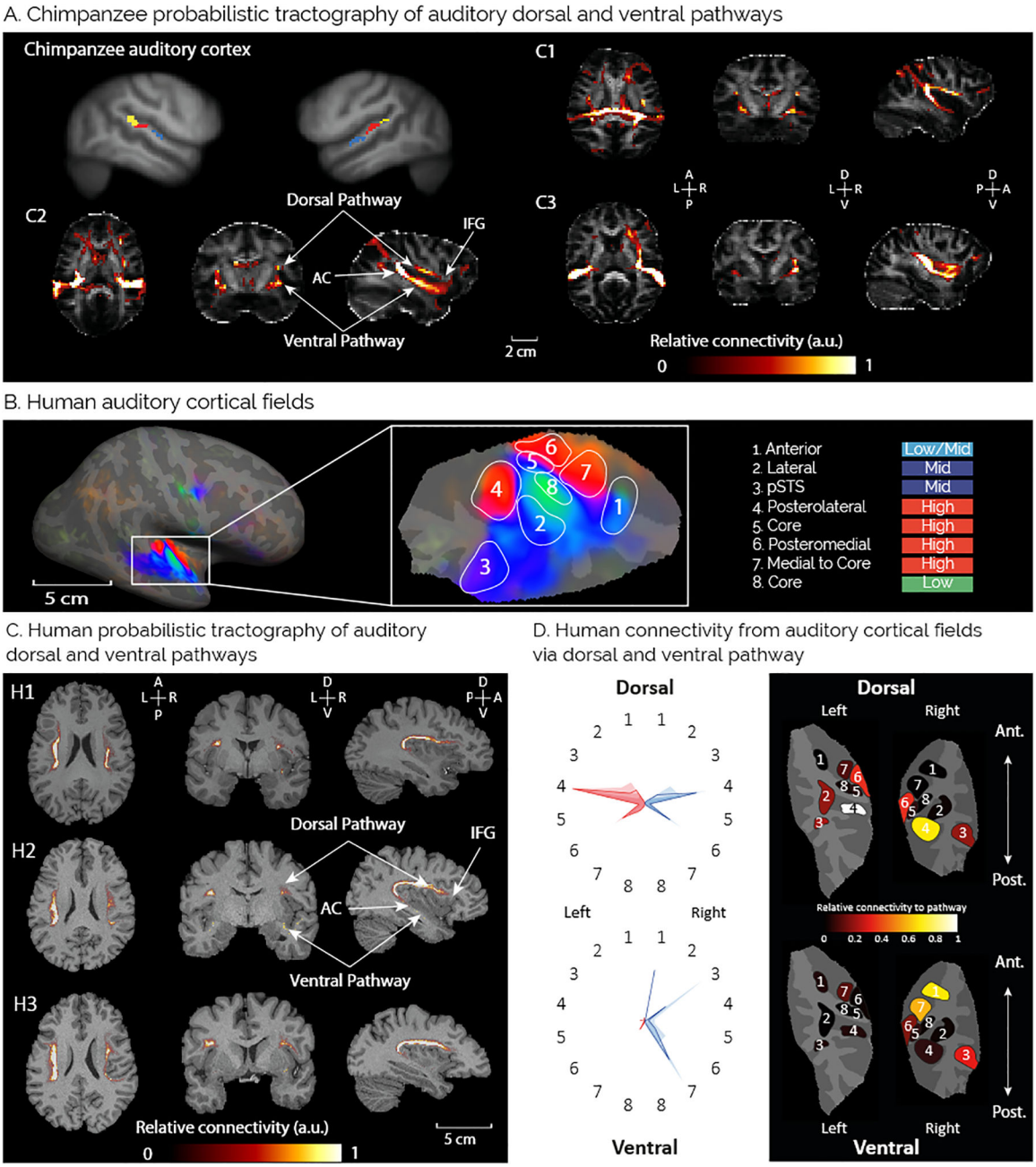

Figure 2. Chimpanzee and human tractography of auditory dorsal and ventral pathways.

(A) Chimpanzee probabilistic tractography between the auditory seed regions and inferior frontal cortex. (B) Tonotopically defined human auditory cortical fields: regions 5 and 8 together may constitute a primary ‘core’ ACF and the surrounding frequency selective areas (1–4 and 6–7) capture at least parts of the adjacent ACFs (Methods). (C) Human probabilistic tractography between the auditory seed regions and inferior frontal cortex. (D) Mean relative connectivity fingerprints (thick lines) and individual variability (shaded) in the left (red) and right hemisphere (blue); shown on ACFs as heat maps (right panel).

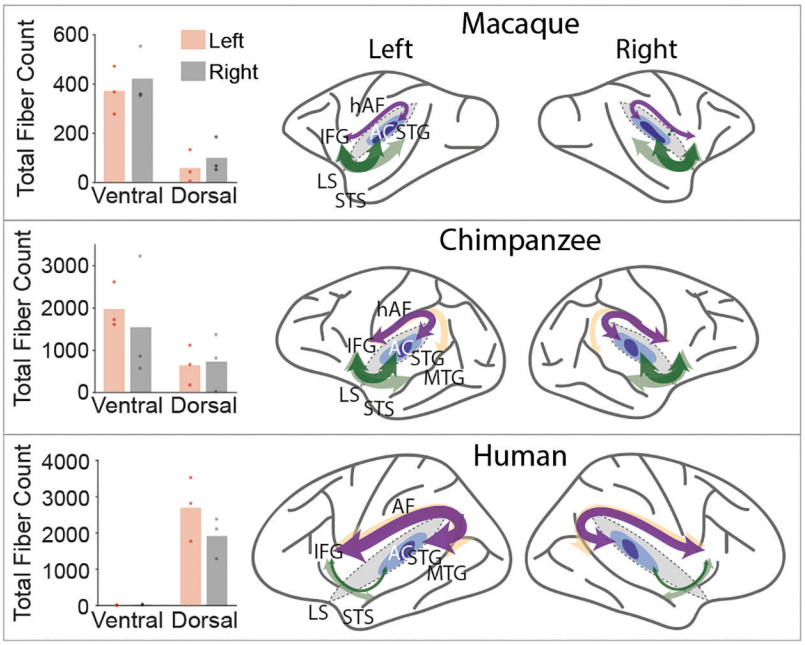

Figure 3. Summary of auditory dorsal and ventral pathway strength and lateralization in macaques, chimpanzees and humans.

Left: Bar plots show individual results and mean fiber counts for the left and right dorsal and ventral pathway for each of the species. Right: schematic summary of the dorsal (purple) and ventral (dark green) pathway results in macaques, chimpanzees and humans, overlaid on prior observations (light yellow and green). Our results replicate key observations from prior studies using other or broader temporal lobe seeds, as follows: stronger *dorsal than ventral* pathway in humans[2,8,10], stronger *ventral than dorsal* pathway in chimpanzees[10], including prominent ventral pathway in macaques[7] and symmetrical ventral pathway (green) in all three species[7,10]. The novel insights into AF evolution stemming from using the functionally defined seeds, are as follows: homologous ventral (dark green) *and* dorsal (purple) pathways from auditory cortex in all three species, with this AF segment left lateralized in humans but not so lateralized in the nonhuman primates. These findings motivate the ***primate auditory prototype*** hypothesis, see text.